IOP Conf. Series: Materials Science and Engineering **231** (2017) 012164 doi:10.1088/1757-899X/231/1/012164

Preparation and characterization of mechanical properties of carbon nanotube reinforced hydroxyapatite composites consolidated by spark plasma sintering

Ye Meng, Wenjiang Qiang and Jingqin Pang

School of Materials Science and Engineering, University of Science and Technology Beijing, Beijing, China

E-mail: mengye2006@qq.com

Abstract. Pure hydroxyapatite(HAP) and 0.5,1,2,3,5wt% carbon nanotubes(CNTs) reinforced HAP which mixed by means of magnetic stirring method were consolidated using a spark plasma sintering(SPS) technique at SPS temperature 1273K, pressure 40MPa, and holding time 5min. The mechanical properties of pure HAP and the composites, such as hardness, flexural strength, and fracture toughness were measured. It is demonstrated that 1wt% of CNTs showed the best performance, which density was 95.78%, the Vickers hardness values was 462HV, flexural strength was 69.2MPa. Enhanced strength and toughness are attributed to the pull-out of CNTs and interfacial bonding mechanism between which and HAP during crack propagation. The flexural strength of the composites with 1 to 3wt% of CNTs were at a high level. When the content of CNTs is excessive, the mechanical properties of the material, especially flexural strength, will decrease quickly.

1.Introduction

Hydroxyapatite (HAP), as one of the most widely used bioactive materials, has attracted considerable attention from materials researcher. HAP has the excellent biocompatibility by means of which is similar to the chemistry of the human bone[1, 6]. HAP provides support for the formation of new bone, and does not cause defensive body reactions. HAP has been used successfully for bone-filling material in dental surgery and orthopedic[2, 8], but its lean mechanical strength limits its applications in load-bearing positions. Pure HAP cannot be used as load-bearing implant because of its poor mechanical properties and reliability. The fracture toughness of the pure dense HAP is 0.8-1.3MPa·$m^{1/2}$, and the flexure strength of it is 38-250MPa, those largely limits the application of HAP[12]. Therefore, it is essential to improve the fracture toughness and flexure strength of HAP.

Iijima found nanoscale needle comprises coaxial tubes of graphitic sheets which produced using an arc-discharge evaporation method in 1991[4]. CNTs have distinctive features, such as electrical conductivity (1.85×103Scm^{-4}), high tensile strength (up to 60GPa)[14], high rigidity (Young's modulus of the order of 1TPa) and large aspect ratio (1000-10000)[7]. These performance given CNTs great advantage in many field of applications, including field emission[10], conductive plastics[5], electrical and thermal conductivity materials, energy storage material and ceramic material[11]. As strengthening phase of ceramic materials, CNTs can improve the mechanical properties of ceramics and improve the toughness of ceramics.

Spark Plasma Sintering(SPS) is a kind of fast, low temperature, energy saving and environmental protection material preparation and processing technology. It is a new technique which directly

applied to the powder particles by DC pulse current, heated by the plasma produced by the spark discharge, sintered in low temperature and short time by means of thermal and field effect[13, 9]. SPS allows the formation of a fine and uniform microstructure in a short period of time through the rapid heating rate by pulsed electrical discharge and high pressure application[3].

In this study, a dispersion of CNTs in HAP powders is attempted using a process of magnetic stirring method. In addition, the consolidation of carbon nanotube reinforced HAP was conducted by SPS. The mechanical properties, including hardness, flexural strength and fracture toughness are measured. A major objective of this work is to evaluate the effect of CNTs content on the mechanical properties of CNTs/HAP composites, thus identifying the optimal processing parameters.

2.Experimental procedures

HAP powder (molecular formula is $Ca_5HO_{13}P_3$) with a purity of 97% and average size less than 200nm was produced by Sigma-Aldrich. Co. USA. Multi-walled carbon nanotubes(MWNTs) were supplied by Shenzhen Nano-Tech. Port Co. Ltd., China, with the dimensions of 10-20nm in diameter and 5-15μm in length. Fig 1 shows the SEM images of HAP powder and MWNTs. The materials used in this study were HAP powder reinforced with different weight fractions of MWNTs (0.5wt%, 1wt%, 2wt%, 3wt%, and 5wt%, respectively). First of all, the corresponding mass of MWNTs was dispersed by ultrasonic wave for 40min in an alcohol solvent. Then added HAP powder, magnetic stirring for 2 hours with the speed of 300rpm, and dried in a drying oven at 343K for 15 hour.

The mixture was pressed into a graphite mould to produce a consolidation by the SPS process (SPS. Dr. Sinter 1050, Sumitomo Coal Mining Co. Ltd., Japan). The powder was loaded into a graphite mould with a 20mm inner diameter. A sheet of graphite paper was placed on the inner wall of the mould to separate the powder and the mould in order to remove easily. The SPS sintering experiments of the samples were conducted at 1273K under vacuum conditions (less than 20Pa). The applied pressure was 10MPa up to 973K and 40MPa at above 1073K. The sintering temperature was increased to 1173K at a rate of 100K/min and then the heating rate was reduced to 50K/min, 30K/min and 20K/min, in turn, until the temperature reached 1273K, with a holding time of 5min. After holding, the applied pressure was reduced to 10MPa by furnace cooling. For comparison, a pure HAP specimen was prepared using the same method. Fig 2 shows the sintering process.

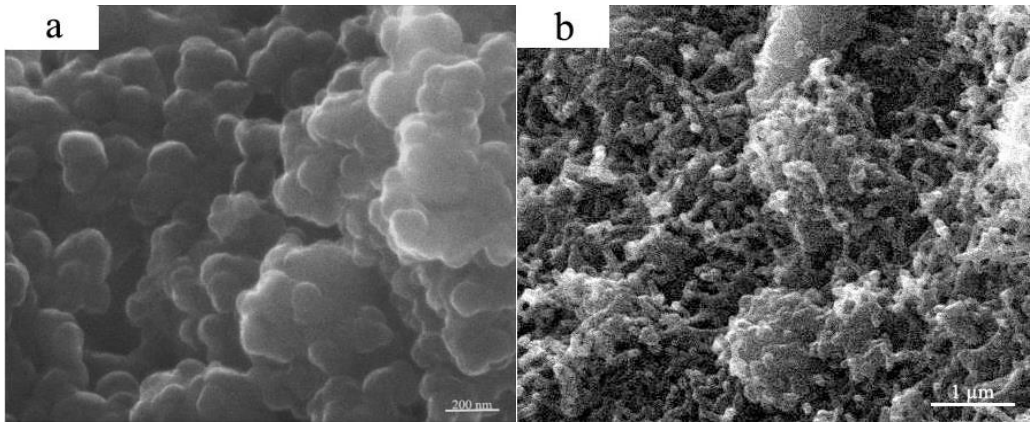

Fig 1. SEM images of raw materials: (a) pure HAP powder and (b) Multi-walled carbon nanotubes.

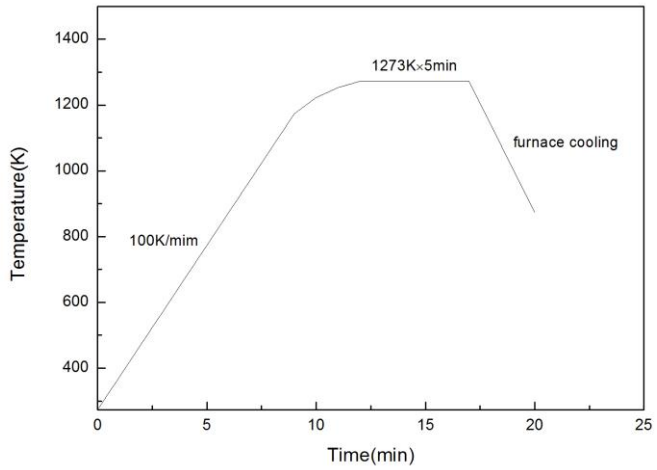

Fig 2. The sintering process by spark plasma sintering.

The crystal structure was identified by the X-ray diffraction (Rigaku Ultima IV) with Cu Kα radiation (λ=1.5406Å) operated at 40kV and 40mA. The microstructures and fractured surfaces were characterized by field emission scanning electron microscopy (FESEM, Zeiss Supra55). Densities of the consolidated composite specimens were obtained by Archimedes method, with distilled water as the intrusion medium. The theoretical densities of HAP (3.14g/cm^3) and CNTs (1.75g/cm^3), provided by the manufacturer, were used to calculate the relative density of composite specimens. The specimens were polished with SiC sand paper and diamond suspension in sequence. Flexural strength test specimens with the dimensions of 2.5mm×2.5mm×18mm were cut from sintered body using a diamond saw. The Vickers hardness and fracture toughness of the test specimens were prepared by a high quality and smoothly polished specimen surface. The indentation on the polished specimens was carried out by using a Vickers pyramidal microhardness indenter (MH-6, Shanghai wujiu automation equipment co., LTD, China) at a load of 300g for hardness and a 2.94N force for fracture toughness for 10s.

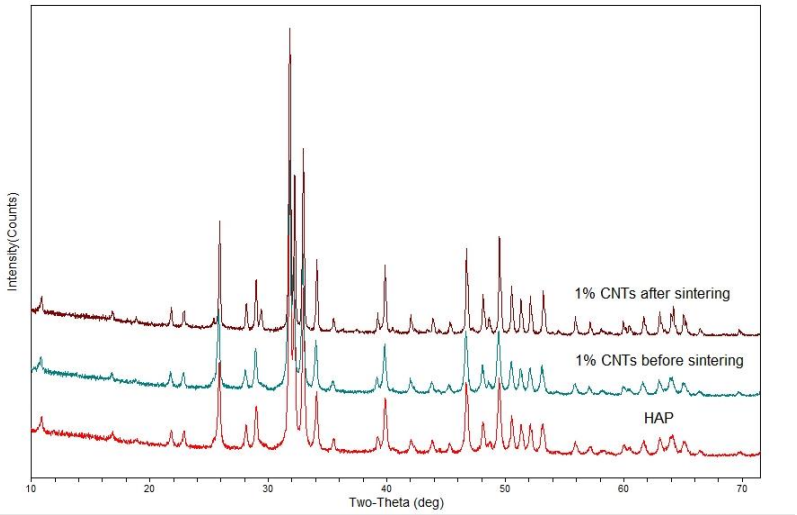

Fig 3. The XRD pattern of HAP and MWNTs/HAP composites before and after sintering.

3. results and discussion

As is shown in fig 3, it is observed that the main phase of the composite is pure HAP (matches with JCPDS PDF #09-0.32), with three most intense peaks corresponded to (211), (300) and (112) planes respectively. No systematic change in the lattice constants is observed whether the composite was before or after sintering.

Fig 4 shows that the axial displacement of the electrodes in the sintering process was a qualitative representation of the densification process of the sintered body. The sintering powder shows a process of expansion when the sintering temperature is below 973K, which shows that there is no densification in the process of thermal expansion of the sintered body at 973K. The axial pressure to the mold is beginning to increase at 973K, at the same time, the axial displacement of the electrodes is beginning to increase, which shows that the sintering body starts to compress under the action of external force. Because of the pressure of the axial pressure, the axial displacement of the electrode cannot be explained by the beginning of the densification process, but the axial pressure is kept constant at 40MPa above 1073K, and the axial displacement of the electrodes is still increasing at the same time, which is the performance of densification. When the sintering temperature reaches 1173K, the axial displacement of the electrodes changed from increased significantly to decreased inconspicuously, which indicates that the densification process of the sintered body has been completed, and there is no change till the end of heat preservation.

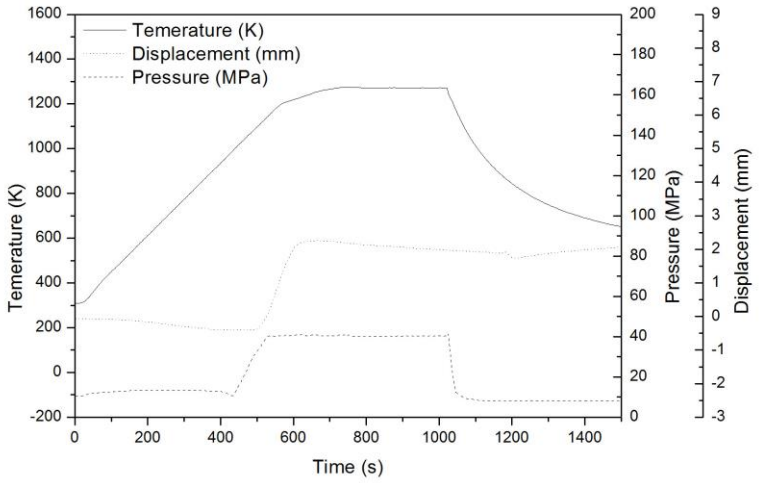

Fig 4. The relationship between temperature, pressure and displacement of SPS sintering.

Under the SPS conditions of sintering temperature 1273K, pressure of 40MPa, and holding time of 5min, in addition to 5wt% MWNTs, the relative density of all the composite materials reached more than 90%, as shown in Table 1. Compared with the pure HAP sintered part, the hardness of MWNTs/HAP composites decreases, it is due to the lower hardness of the MWNTs phase compared with the HAP matrix and the increase of the agglomeration.

Table 1. The resultant mechanical properties of the sintered MWNTs/HAP composites

Materials	Relative density (%)	Flexural strength (MPa)	Hardness (HV)	Fracture toughness ($MPam^{1/2}$)
HAP	96.34	28±10	562±12	0.8±0.04
0.5wt%MWNTs	94.76	62.8±8	497±7	1.54±0.05
1wt% MWNTs	95.78	69.2±6	462±10	1.56±0.08
2wt% MWNTs	94.73	62.3±6	452±8	1.76±0.12
3wt% MWNTs	91.12	61.5±9	448±7	1.83±0.09
5wt% MWNTs	88.71	43.3±5	390±11	1.85±0.10

The density of the sintered body was obviously decreased with the increase of MWNTs content. The main reason is that the MWNTs are easy to agglomerate. When the content was high, the dispersion of MWNTs decreased, resulting in agglomeration which reduce the density of the sintered body.

Fig 5 shows that with the increase of the content of the MWNTs, the flexural strength of the sintered body increases first and then decreases, and reaches the highest at 1wt% MWNTs. The flexural strength of the composite sintered with MWNTs was higher than that of pure HAP. The interfacial bonding was enhanced with the addition of MWNTs which also generate the pullout mechanism. The strengthening effect of MWNTs decreases with a further increase when the MWNTs weight fraction is greater than 1wt%. This is because the dispersion of MWNTs in the matrix is poor, and the agglomeration of MWNTs weakens the bonding between MWNTs and HAP.

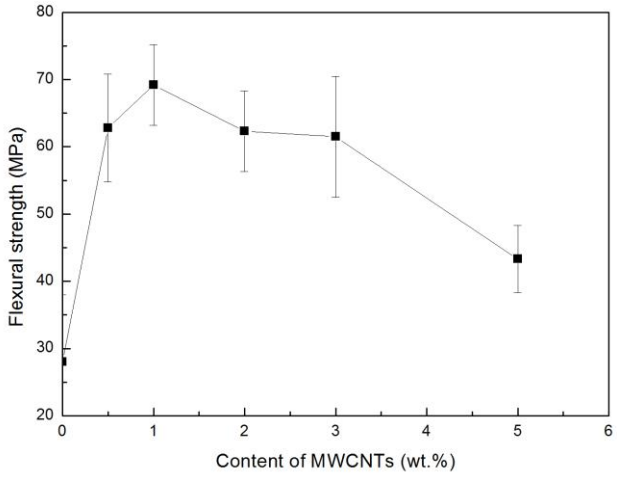

Fig 5. Flexural strength of MWNTs/HAP composites as a function of MWNTs (wt%)

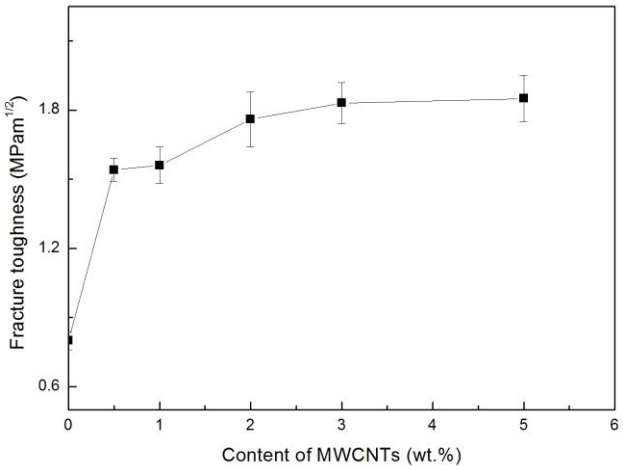

Fig 6. Fracture toughness of MWNTs/HAP composites as a function of MWNTs (MPa·m$^{1/2}$)

Fig 6 shows the relationship between the fracture toughness of composites and the weight fraction of MWNTs. The fracture toughness of the composite sintered with MWNTs was higher than that of

pure HAP. This is attributed to the dispersion of MWNTs in the matrix, which serves as a reinforcing phase. HAP was reinforced by toughening mechanisms, such as pull-out by the MWNTs.

The fracture morphology of the composites, obtained by flexural strength tests, are shown in Fig 7. Fig 7 shows the pull-out toughening of the MWNTs in the fractured surface of the MWNTs/HAP composites. Therefore, an improvement in mechanical properties can be predicted by the toughening mechanism. In Fig 7(a), MWNTs were dispersed homogeneously in HAP matrix. The pull-out MWNTs and residual holes left by MWNTs indicated the crack deflection and the pullout mechanism. Any solid material under the action of the load, the way to absorb energy is nothing more than two ways: material deformation and the formation of a new surface. For brittle matrix, the deformation is very small, so the absorption of the fracture energy is also rare. In order to improve the energy absorption of this kind of material, it can only increase the fracture surface, that is to increase the crack propagation path. Brittle materials can be toughened by the addition of the second phase materials such as fibers, provided crack deflection occurs at the interfaces between the fibers and the matrix. On the other hand, agglomerates of undispersed MWNTs were found in Fig 7(b) which shows the fracture surface of the composites with 5wt%, and were always accompanied by large pores caused by the agglomeration of MWNTs, which resulted in lower relative density of the composites.

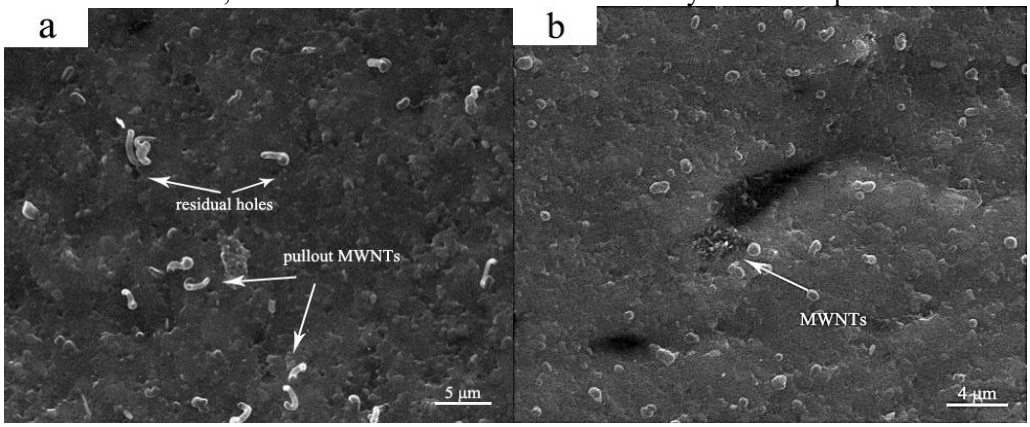

Fig 7. SEM images of fracture surfaces of the composites: (a) 1wt% MWNTs/HAP composite and (b) 5wt% MWNTs/HAP composite.

4.conclusions

Pure hydroxyapatite (HAP) and 0.5,1,2,3,5wt% carbon nanotube reinforced HAP which mixed by means of magnetic stirring method were consolidated using a spark plasma sintering(SPS) technique at SPS temperature 1273K, pressure 40MPa, and holding time 5min. The optimal content of MWNTs in the composites is 1wt%. The hardness of composites decreased appreciably compared with the HAP matrix. The flexural strength and fracture toughness increased 147% (up to 69.2MPa) and 95% (up to 1.56MPam$^{1/2}$). MWNTs are good candidates as reinforcement for strengthening HAP matrix composites. The MWNTs/HAP composites can be used as scaffold matrix materials in bone tissue engineering.

References

[1] Ankur G, Garima T, Debrupa L and Kantesh B 2013 Compression Molded Ultra High Molecular Weight Polyethylene-Hydroxyapatite-Aluminum Oxide-Carbon Nanotube Hybrid Composites for Hard Tissue Replacement J MATER SCI TECHNOL 514-22

[2] Barakat N A M, Khalil K A, Sheikh F A, Omran A M, Gaihre B, Khil S M and Kim H Y 2008 Physiochemical characterizations of hydroxyapatite extracted from bovine bones by three different methods: Extraction of biologically desirable HAp Materials Science and Engineering: C 28 1381-7

[3] El-Hadek M A Œ K 2013 Fracture Properties of SPS Tungsten Copper Powder Composites Metallurgical and Materials Transactions A 44 544-51
[4] Iijima S 1991 Helical microtubules of graphitic carbon NATURE 354 56-8
[5] Kang S J, Song Y, Yi Y, Choi W M, Yoon S and Choi J 2010 Work-function engineering of carbon nanotube transparent conductive films CARBON 48 520-4
[6] Kealley C, Elcombe M and van Riessen A 2008 Microstrain in hydroxyapatite carbon nanotube composites J SYNCHROTRON RADIAT 15 86-90
[7] Kumari L, Zhang T, Du G H, Li W Z, Wang Q W, Datye A and Wu K H 2009 Synthesis, microstructure and electrical conductivity of carbon nanotube–alumina nanocomposites CERAM INT 35 1775-81
[8] Lee B, Lee C, Gain A K and Song H 2007 Microstructures and material properties of fibrous HAp/Al2O3–ZrO2 composites fabricated by multi-pass extrusion process J EUR CERAM SOC 27 157-63
[9] Makino Y, Mizuuchi K, Tokita M, Agari Y, Kawahara M and Inoue K 2010 Synthesis of New Structural and Functional Materials by SPS Processing Materials Science Forum 638-642 2091-6
[10] Park J, Kim J, Noh Y, Jo K, Lee S, Choi H and Kim J 2010 X-ray images obtained from cold cathodes using CNTs coated with gallium-doped zinc oxide thin films THIN SOLID FILMS 519 1743-8
[11] Patil S S, Koinkar P M, Dhole S D, More M A and Murakami R 2011 Influence of high-energy electron irradiation on field emission properties of multi-walled CNTs (MWCNTs) films Physica B: Condensed Matter 406 1809-13
[12] Rapacz-Kmita A, Lósarczyk A and Paszkiewicz Z 2006 Mechanical properties of HAp–ZrO2 composites J EUR CERAM SOC 26 1481-8
[13] Tokita M 2010 The Potential of Spark Plasma Sintering (SPS) Method for the Fabrication on an Industrial Scale of Functionally Graded Materials Advances in Science and Technology 63 322-31
[14] Zaman A C, Üstündağ C B, Çelik A, Kara A, Kaya F and Kaya C 2010 Carbon nanotube/boehmite-derived alumina ceramics obtained by hydrothermal synthesis and spark plasma sintering (SPS) J EUR CERAM SOC 30 3351-6